Local density of states and modes of circular photonic crystal cavities

Jiří Chaloupka,[1] Javad Zarbakhsh,[2] and Kurt Hingerl[2,*]

[1]*Department of Solid State Physics, Institute of Condensed Matter Physics, Faculty of Science, Masaryk University, Kotlářská 2, CZ-61137 Brno, Czech Republic*

[2]*Christian Doppler Labor für Oberflächenoptische Methoden, Institut für Halbleiter und Festkörperphysik, Universität Linz, A-4040 Linz, Austria*

Because the penetration depth of light in the band gap is of the order of one lattice constant of a photonic crystal, structures such as circular photonic crystals (CPC) confine light. We show that an extension of the CPC concept to holes in any high-index material yields confinement only in the case that the hole size is varied jointly. Applying the Bloch-Floquet theorem in such a rotationally symmetric case leads to a decomposition of the Green's tensor. By using the photonic local density of states (LDOS) components in a CPC, the eigenfrequencies of localized cavity modes can be efficiently found.

I. INTRODUCTION

Photonic band-gap materials are artificial structures with spatial variation of permittivity. For quite a long term, periodicity has been considered as an essential requirement for the formation of a photonic band gap. Investigations on photonic quasicrystals,[1] curvilinear photonic crystals,[2] and circular photonic crystals[3] (CPC) have changed this view. CPCs proposed and investigated by Horiuchi *et al.*[3] consist of alumina rods of constant radii arranged in concentric circles. The distance between rods on each concentric circle was kept constant as well as the difference between radii of adjacent circles. It was shown that such CPCs have isotropic photonic gaps. However, the papers cited above find *complete* band gaps in these two-dimensional structures only for the case of dielectric rods in air and not for air holes in a dielectric material. For airholes with constant size in a dielectric material complete photonic band gaps do not form because the necessary lattice distortion does not preserve the gap. This can best be proved by using the reasoning of Ref. 2: In order to construct a circular photonic crystal, a lattice distortion changing the local symmetry from hexagonal to square, passing through a rhombic structure, is necessary. By plotting the band-gap map for the transition towards a square structure it is immediately seen that the width of the band gap is strongly reduced and confinement vanishes. This is mainly due to the properties of the square-lattice band gap of a structure with holes in a high-index material. Therefore within this article a further degree of freedom, *the variation of the structure—i.e., hole size—* is introduced, which allows us to keep huge band gaps.

In the presence of a photonic band gap (PBG) the modes can be confined within a well-constructed microcavity[2,4,5] promising various applications, such as microscopic lasers.[6] Eigenmodes of photonic cavities and other defects were calculated using a number of methods, e.g., plain-wave expansion and the finite-difference time-domain method. Recent works show that the local density of states (LDOS) is a suitable tool to investigate the confinement of modes in various cavities.[7] The LDOS is directly connected to the emission rate of an embedded point source at a given position, for

example, an excited atom. For a cavity in an infinite structure, the LDOS vanishes within the band gap, and therefore spontaneous emission is inhibited. When the transition frequency approaches some eigenfrequency of the cavity, the rate of spontaneous emission can be extremely increased. The LDOS can be conveniently obtained from the electromagnetic Green's tensor of the photonic crystal. In the case of two-dimensional photonic crystals consisting of dielectric cylinders, the exact theory of multipole expansions is well suitable for calculation of the Green's tensor.[8]

In this paper we introduce a class of PBG structures, where we vary not only the periodicity but also the size of dielectric holes/rods, in order to construct scattering arrangements which confine the light for the case of airholes in dielectrics, named *variable-size CPC* (VSCPC). The formation of VSCPC is brought up by the question: Which pair combinations of hole radii versus hole distances form a stop band at a given frequency? Such an approach is meaningful, provided that the penetration depth of light in the band gap is less or of the order of one lattice constant of a photonic crystal. Then changes in the subsequent layers yielding the same band gap will give an additional freedom in constructing VSCPC. This question on the combinations of hole radii versus hole distances can best be answered by looking at band-gap maps (stop-band frequencies vs period) as displayed in the inset of Fig. 1 for the case of the transverse-electric (TE) polarization (H_z component). Using the scaling properties of the Maxwell equations and fixing the vacuum wavelength λ_0 at 1.55 μm this band-gap map can be immediately converted into the curve indicated by 0% gap rate in the main plot of Fig. 1. In the same figure the contour plots for 10% and 25% gap rate (width of stop band/midgap frequency) are shown, together with the straight line indicating the touching of the etched holes. This freedom in construction is justified by two facts: (i) the penetration depth of light in the band gap is of the order of one lattice constant,[2] and (ii) the band-gap maps exhibit band gaps for different radius/period ratios,[9] so taking into account the previous argument, radius and period must be varied jointly for building a band gap at a given frequency. An example of a 16-fold VSCPC can be seen in Fig. 5, where this additional freedom has been
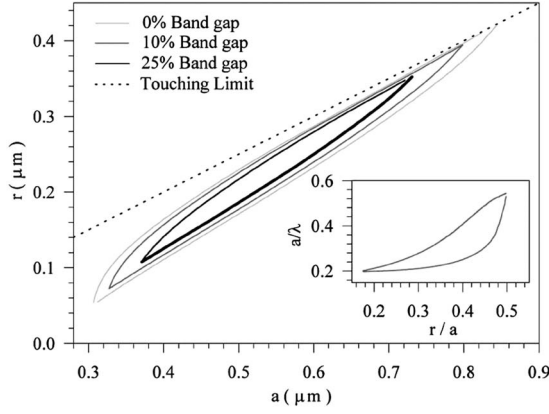
FIG. 1. Gap-rate equicontour plot showing the pair values of hole radius versus distance for a hexagonal structure of air holes in silicon ($n=3.4$). H_z polarized light with $\lambda_0=1.55$ μm assumed. The inset shows stop-band frequencies vs relative radius.

used and so a structure similar to a hexagonal one can be kept.

II. THEORY

For the investigation of the VSCPC structures, in the following we provide an efficient method based on multipole expansions taking advantage of symmetry in a VSCPC. Let us consider a general case of a two-dimensional VSCPC possessing N-fold rotational symmetry around the z axis.

The electromagnetic wave can be decomposed into two independent polarization states (determined by E_z, also called TM, or H_z, also called TE). We assume that the time dependence is of the form $e^{-i\omega t}$ for all the fields. For the H_z polarization, the eigenmodes obey the following equation:

$$\hat{\mathcal{H}}_{\text{TE}} H_z(\mathbf{r}) = \frac{\omega^2}{c^2} H_z(\mathbf{r}), \tag{1}$$

where $\hat{\mathcal{H}}_{\text{TE}}$ is the Hermitian operator

$$\hat{\mathcal{H}}_{\text{TE}} = - \nabla \frac{1}{\epsilon(\mathbf{r})} \nabla . \tag{2}$$

For the case of the E_z polarization, we introduce the field $Q_z(\mathbf{r}) = \sqrt{\epsilon(\mathbf{r})}[E_z(\mathbf{r})]$. Then, the eigenmode equation for Q_z contains a Hermitian operator of the form

$$\hat{\mathcal{H}}_{\text{TM}} = - \frac{1}{\sqrt{\epsilon(\mathbf{r})}} \nabla^2 \frac{1}{\sqrt{\epsilon(\mathbf{r})}} . \tag{3}$$

Due to the N-fold rotational symmetry of the permittivity, both these operators commute with the unitary operator $\hat{\mathcal{R}}_{2\pi/N}$ of an elementary rotation through the angle $2\pi/N$. A pair of commuting operators, one Hermitian and the other unitary, can be simultaneously diagonalized. Therefore, it is possible to obtain the set of eigenfunctions satisfying

$$\hat{\mathcal{R}}_{2\pi/N} Q_{zn}(\mathbf{r}) = e^{-iK_n(2\pi/N)} Q_{zn}(\mathbf{r}), \tag{4}$$

where $Q_{zn}(\mathbf{r})$ denotes the nth eigenmode of $\hat{\mathcal{H}}_{\text{TM}}$ (and equivalently for H_z). Equation (4) represents a rotational

analogy of the well-known Bloch-Floquet theorem in the theory of crystalline solids. Thus, we call K the rotational Bloch number. Uniqueness of the field with respect to full rotation through 2π requires K to be an integer. It is sufficient to take the rotational Bloch number from the set $\{0, 1, 2, \ldots, N-1\}$. The consequences of Eq. (4) may be demonstrated using an analogy with the electronic bands of a perfect crystal. Instead of a continuous quantum number (e.g., Bloch vector $\mathbf{k}$) as it shows up in the case of the infinite translational periodicity, the modes are now classified using a discrete quantity (rotational Bloch number), which is a consequence of the discrete rotational symmetry with finite N. This leads to a finite number of eigenmodes confined within the VSCPC structure compared to the continuum of electronic states in a perfect crystal.

The eigenmodes appear as resonances in the frequency dependence of the power radiated by a virtual oscillating dipole moment[10] or as peaks in the frequency dependence of the LDOS. Because of the direct connection between the LDOS and the emission rate of a dipole source,[11] both methods to find eigenfrequencies are equivalent. We will adopt the latter one and use the electric Green's tensor G^e to calculate the corresponding LDOS ρ via[12]

$$\rho(\mathbf{r};\omega) = - \frac{2\omega}{\pi c^2} \text{Im}[\text{Tr } \mathbf{G}^e(\mathbf{r},\mathbf{r};\omega)]. \tag{5}$$

The Green's tensor can be split for the two polarizations, and its calculation involves solution of three scalar problems,[8] namely finding Green's functions of the Hermitian operator $\hat{\mathcal{H}} = \nabla^2 + n^2(\mathbf{r})\omega^2/c^2$, which commutes with $\hat{\mathcal{R}}_{2\pi/N}$. In the case of the E_z polarization the two-dimensional Green's function satisfies the equation

$$\hat{\mathcal{H}} G(\mathbf{r},\mathbf{r}_s) = \delta(\mathbf{r} - \mathbf{r}_s), \tag{6}$$

representing Green's problem with a monopole source, whereas for the H_z polarization the righthand side contains dipole source contributions $-\partial_y\delta(\mathbf{r}-\mathbf{r}_s)$ and $\partial_x\delta(\mathbf{r}-\mathbf{r}_s)$, respectively.[8] In addition to Eq. (6), boundary conditions for the appropriate polarization have to be satisfied.

Equation (4) raises the question: How it is possible to separate contributions of different K values in the optical response of the VSCPC to be able to classify the eigenmodes according to their rotational Bloch numbers? This can be achieved by performing Fourier analysis with respect to the angular coordinate. For this purpose we define the operator

$$\hat{\mathcal{F}}_K = \frac{1}{N} \sum_{j=0}^{N-1} e^{iK(2\pi j/N)} \hat{\mathcal{R}}_{2\pi/N}^j, \tag{7}$$

which acting on an arbitrary function produces a function satisfying Eq. (4). Applying this operator, we can transform Eq. (6) into set of N independent equations for the K components of the Green's function defined by $G_K(\mathbf{r},\mathbf{r}_s) = \hat{\mathcal{F}}_K G(\mathbf{r},\mathbf{r}_s)$. This set reads
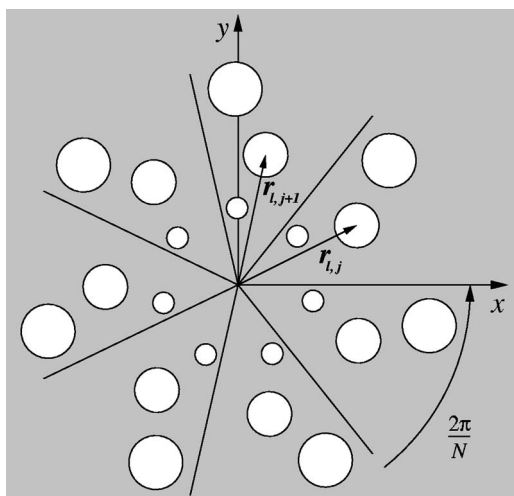
FIG. 2. Two-dimensional circular photonic crystal with seven-fold rotational symmetry consisting of three rings. Center positions of two neighboring cylinders in the same ring are labeled by $r_{l,j}$ and $r_{l,j+1}$.

$$\hat{\mathcal{H}}G_K(r,r_s) = \hat{\mathcal{F}}_K[\delta(r - r_s)], \quad K = 0,1,\ldots,N-1. \quad (8)$$

The LDOS components corresponding to different values of K are then calculated by means of Eq. (5) with Tr G^e replaced by G_K. In these components resonant peaks are expected at the eigenfrequencies of modes with matching rotational Bloch number. The case of dipole sources for the H_z polarization can be treated in a similar way.

Using the identity operator expressed in terms of $\hat{\mathcal{F}}_K$ for all rotational Bloch numbers $\sum_{K=0}^{N-1}\hat{\mathcal{F}}_K = \hat{\mathcal{I}}$, it is also possible to obtain the complete Green's function from the set of its K components

$$G(r,r_s) = \sum_{K=0}^{N-1} G_K(r,r_s). \quad (9)$$

The same relation holds between the complete LDOS and its K components.

So far, our considerations have required only N-fold rotational symmetry of the system. Now we assume a more special case of a VSCPC consisting of N_{ring} rings of dielectric rods positioned in the background medium with the refractive index n_0. Each ring consists of N cylinders with the same radii and refractive indices. An example of such a structure is presented in Fig. 2.

The cylinders in the VSCPC are labeled by $r_{l,j}$, where the first index indicates the number of the ring and the second one the number of the segment, ranging from $j=0$ to $j=N-1$. The mutual relation between the positions of the cylinders on the same ring is given by $r_{l,j} = \hat{\mathcal{R}}_{2\pi/N}^j[r_{l,0}]$. Next, we introduce the local polar coordinate system $(r_{l,j}, \theta_{l,j})$ with origin at $r_{l,j}$.

Since the structure consists of cylinders, it is convenient to use the multipole expansion method of Ref. 8 modified for our case. We restrict ourselves to the E_z polarization and the source positioned outside the cylinders. In other cases, similar modifications have to be performed. In order to guarantee

Eq. (4) and Eq. (8), we write the K-component of the Green's function as the multiple multipole expansion

$$G_K(r,r_s) = \hat{\mathcal{F}}_K\left[\frac{1}{4i}H_0^{(1)}(n_0k|r - r_s|) \right.$$
$$\left. + \sum_{l=1}^{N_{\text{ring}}} \sum_{p=-\infty}^{\infty} B_p^l H_p^{(1)}(n_0 k r_{l,0})e^{ip\theta_{l,0}} \right], \quad (10)$$

where $H_p^{(1)}$ are the outgoing Hankel functions and $k=\omega/c$. The multipole coefficients B_p^l have to be chosen in such a way that the boundary conditions are satisfied at the surface of each cylinder. Following the procedure in Ref. 8, i.e., applying Graf's addition theorem and comparing resulting expansions, we obtain a linear system determining the multipole coefficients

$$M_p^l B_p^l + \sum_{q=1}^{N_{\text{ring}}} \sum_{m=-\infty}^{\infty} B_m^q \sum_{j=0,(q,j)\neq(l,0)}^{N-1} e^{i(K-p)(2\pi j/N)}$$
$$\times H_{p-m}^{(1)}(n_0 k r_{l0,qj})e^{i(m-p)\theta_{l0,qj}}$$
$$= -\frac{1}{4i}\sum_{j=0}^{N-1} e^{iK(2\pi j/N)}H_p^{(1)}(n_0 k r_{l0,sj})e^{-ip\theta_{l0,sj}}, \quad (11)$$

where M_p^l has the same definition as in Ref. 13. We have also introduced quantities $r_{l0,qj}$ and $\theta_{l0,qj}$ denoting the relative position $r_{q,j} - r_{l,0}$ expressed in polar coordinates. Finally, $r_{l0,sj}$ and $\theta_{l0,sj}$ correspond to $\hat{\mathcal{R}}_{2\pi/N}^j[r_s] - r_{l,0}$.

III. RESULTS AND DISCUSSION

As a first example we present a 12-fold VSCPC of silicon rods ($\epsilon=11.6$) in air for the E_z polarization. In Fig. 3(a) the complete LDOS as well as the its $K=0$ component is plotted in reduced form $\pi c^2 \rho/2\omega$. The frequency dependence of the complete LDOS, especially its huge reduction for a range of frequencies by 2–5 orders of magnitude, clearly reflects the presence of the band gap—approximately between $\omega a/c=1.3$ and $\omega a/c=2.3$. Several peaks corresponding to localized modes appear within the band gap. In this particular case, the number of the confined modes is small due to the small cavity radius compared to the wavelengths of the gap. Fig. 3(a) is also a graphical representation of Eq. (9). For instance the peak in the complete LDOS at $\omega a/c \approx 1.9$ is mainly determined by the $K=0$ component. Figures 3(b)–3(e) show field distributions of localized modes with $K=0$, 1, 2, and 3 related to the peaks labeled in Fig. 3(a). The field distributions were computed using the corresponding component of the Green's function, since the other components are negligible for a resonant mode. Please note that for the high-index rods as in this example a joint variation of hole size and distance is not necessary in order to preserve the band gap, nevertheless this structural freedom can be used as shown in Fig. 3(b)–3(e).

The field distributions can be roughly estimated when regarding the VSCPC as a circular resonant cavity surrounded by an impenetrable wall. The eigenmodes in this case are proportional to $J_m(n_0 k r)e^{im\varphi}$. The modes with m
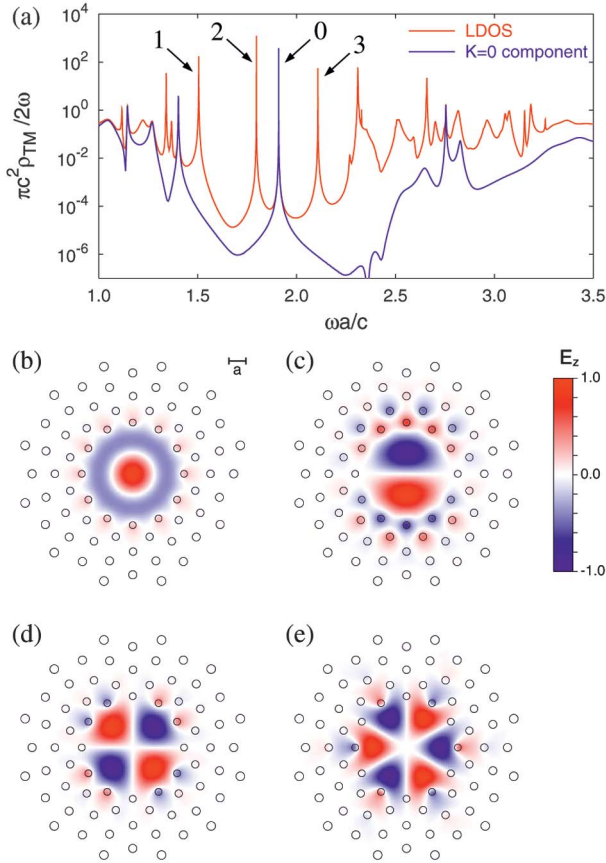
FIG. 3. (Color) (a) Complete LDOS and its $K=0$ component at the point with coordinates $x=1.0a$ and $y=0.2a$. Distribution of the electric fields: (b) $K=0$ mode, (c) $K=1$, (d) $K=2$, (e) $K=3$.

$=K\pm N, K\pm 2N, \dots$ correspond to the rotational Bloch number K. The eigenfrequencies are determined by the boundary condition at the inner surface of the cavity, i.e., $J_m(n_0 kR) = 0$, where R is the cavity radius. In our case the dielectric holes form such an impenetrable wall for a range of frequencies. The effective cavity radius corresponds approximately to the radius of the first ring.

To discuss the symmetry of the modes, we use the group theory. The symmetry group C_{12v} of our system consists of nine classes of conjugate elements

$$C_{12v} = \{E, 2C_{12}, 2C_6, 2C_4, 2C_3, 2C_{12}^5, C_2, 6\sigma_x, 6\sigma_d\}.$$

Together with the rotations, there are 12 mirror planes. Due to this additional symmetry, the rotational Bloch numbers K and $12-K$ are equivalent. The group C_{12v} has four one-dimensional irreducible representations A_1, A_2, B_1, B_2. The A representations correspond to $K=0$, whereas the B representations correspond to $K=6$ (or, generally, to $K=N/2$ for any even N). The other rotational Bloch numbers are related to the two-dimensional irreducible representations $E_1 - E_5$. As a consequence, the $K=0$ mode in Fig. 3(b) is nondegenerate while the modes with $K=1$, 2, and 3 are doubly degenerate.

As a second example, we study a 16-fold VSCPC consisting of ten rings of air holes in silicon, locally resembling a triangular arrangement. The distance between cylinders and their radii are chosen in such a way that the equivalent infi-
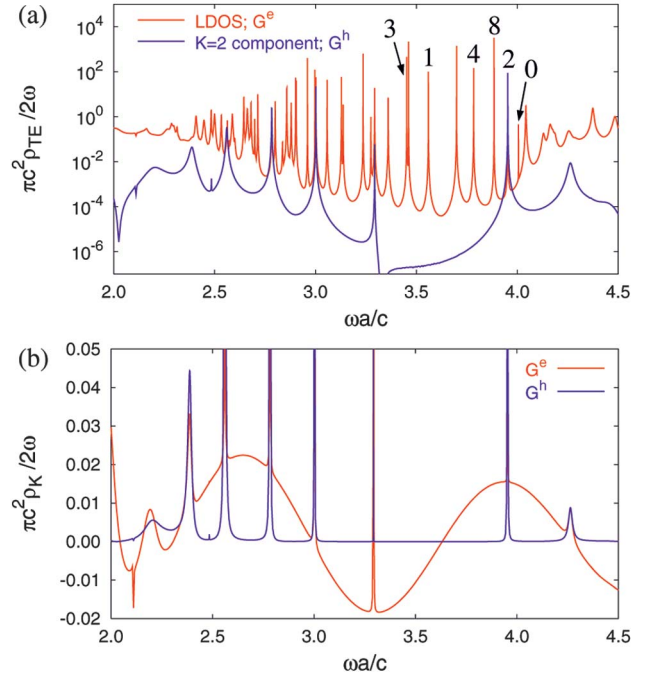

FIG. 4. (Color) (a) Complete LDOS calculated from G^e and the $K=2$ component of the LDOS corre- sponding to G^h. (b) Comparison of $K=2$ components related to G^e and G^h. The first one shows a slowly oscillating background. The curves are calculated for the point with coordinates $x=0.70a$ and $y=0.25a$.

nite hexagonal structure inhibits a certain frequency range of H_z polarized light. Figures 4 and 5 show the LDOS calculations for a randomly chosen point inside the cavity and field distributions of localized modes within the cavity. In Fig.
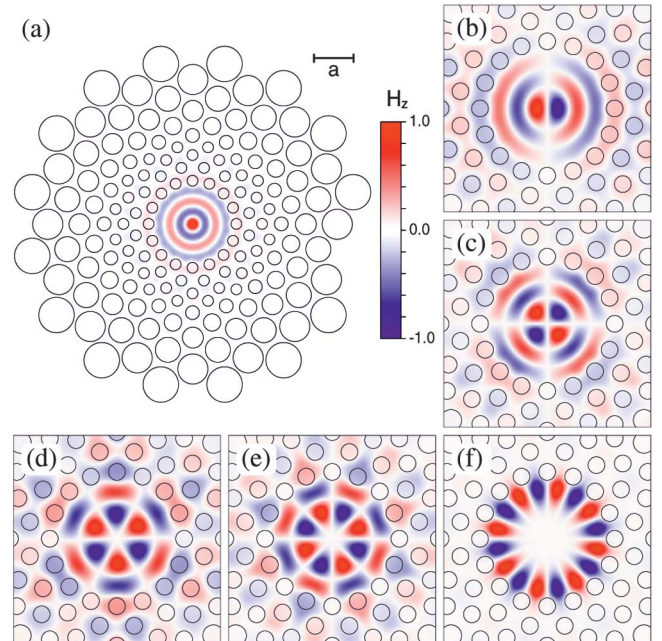

FIG. 5. (Color) Distribution of the magnetic fields: (a) Our sample structure with $K=0$ mode; (b) $K=1$; (c) $K=2$; (d) $K=3$; (e) $K=4$; (f) $K=8$ mode representing a well-localized whispering-gallery mode. The field distribution of degenerated modes is affected by the position of the source.

4(a) we plot the complete LDOS resulting from G^e and the $K=2$ component of the LDOS corresponding to the magnetic Green's tensor G^h. The peaks are closely spaced in the complete LDOS, and therefore it is hard to distinguish them. In contrast to the complete LDOS, the $K=2$ component contains only peaks for this rotational Bloch number K. The reason why we intermix the electric and magnetic G follows.

For the H_z polarization numerical difficulties arise in determining the eigenfrequencies of G^e. A possibility to detect even small changes of the LDOS component in the vicinity of sharp peaks is important to achieve computational efficiency. Then, we can use sparser sampling of the frequencies and avoid missing some of the peaks. The slowly oscillating background of the LDOS component caused by dipole source contributions in Eq. (8) presented in Fig. 4(b) disables this detection. In order to find the resonant frequencies, we have used the LDOS resulting from the magnetic Green's tensor G^h, instead of G^e. The corresponding LDOS for the H_z polarization can be calculated from the solution of Eq. (6), where G satisfies the boundary conditions for H_z field. Its K components do not contain any disturbing background and for our purpose they are preferable to K components related to G^e.

We have selected several peaks corresponding to localized modes. These are labeled in Fig. 4(a) according to their rotational Bloch number K. In Fig. 5, the mode profiles are shown for the selected modes. All the modes are well-localized inside the cavity. The strongest localization is shown by the mode with rotational Bloch number $K=8$ representing a whispering-gallery mode[14] localized near the first ring of holes. This behavior follows from the approximate form of the solution $J_K(n_0kr)e^{iK\varphi}$. The radial part rises as r^K for small r, which makes a larger central hollow for larger K, as can be observed in the sequence Figs. 5(d)–5(f). The eigenmodes are degenerate with the exception of the whispering-gallery mode and the completely symmetric mode with $K=0$. Note also, that the large permittivity of silicon reduces the wavelength, so that the modes have more radial nodes and their number increased in comparison with the previous example.

IV. CONCLUSION

In conclusion, we have shown how to construct CPC and VSCPC cavities, which can support well-localized modes with high-quality factors. Eigenmode frequencies are obtained as the positions of the peaks in the frequency-dependent decomposed LDOS with highly efficient numerical technique taking advantage of the rotational symmetry to reduce the number of multipole coefficients by a factor of N. This considerably reduces the required CPU time and improves accuracy of the solution. Although rotational symmetry other than 2-, 3-, 4-, and 6-fold is prohibited for crystals, our technique could be also applicable for quasicrystals, where any order of rotational symmetry is possible. Possible applications such as waveguiding with arbitrary-angle waveguide bends will be discussed in forthcoming papers.

*Corresponding author: kurt.hingerl@jku.at

[1] Y. S. Chan, C. T. Chan, and Z. Y. Liu, Phys. Rev. Lett. **80**, 956 (1998); T. Janssen, Phys. Rep. **168**, 55 (1988); C. Jin, B. Cheng, B. Man, Z. Li, D. Zhanga, S. Ban, and B. Sun, Appl. Phys. Lett. **75**, 1848 (1999); M. E. Zoorob, M. D. B. Charlton, G. J. Parker, J. J. Baumberg, and M. C. Netti, Nature (London) **404**, 740 (2000); M. A. Kaliteevski, S. Brand, R. A. Abram, T. F. Krauss, P. Millar, and R. M. De La Rue, J. Phys.: Condens. Matter **13**, 10459 (2001); Y. Wang, B. Cheng, and D. Zhang, *ibid.* **15**, 7675 (2003).

[2] J. Zarbakhsh, F. Hagmann, S. F. Mingaleev, K. Busch, and K. Hingerl, Appl. Phys. Lett. **84**, 4687 (2004).

[3] N. Horiuchi, Y. Segawa, T. Nozokido, K. Mizuno, and H. Miyazaki, Opt. Lett. **29**, 1084 (2004).

[4] Y. Akahane, T. Asano, B. S. Song, and S. Noda, Nature (London) **425**, 944 (2003).

[5] H. Benisty, C. Weisbuch, D. Labilloy, M. Rattier, C. J. M. Smith, T. F. Krauss, R. M. De La Rue, R. Houdré, U. Oesterle, C. Jouanin, and D. Cassagne, J. Lightwave Technol. **17**, 2063 (1999).

[6] O. Painter, R. K. Lee, A. Scherer, A. Yariv, J. D. O'Brien, P. D. Dapkus, and I. Kim, Science **284**, 1819 (1999).

[7] I. Bulu, H. Caglayan, and E. Ozbay, Phys. Rev. B **67**, 205103 (2003).

[8] A. A. Asatryan, K. Busch, R. C. McPhedran, L. C. Botten, C. M. de Sterke, and N. A. Nicorovici, Waves Random Media **13**, 9 (2003).

[9] J. D. Joannopoulos, R. D. Meade, and J. N. Winn, *Photonic Crystals: Molding the Flow of Light* (Princeton University Press, Princeton, 1995).

[10] K. Sakoda and H. Shiroma, Phys. Rev. B **56**, 4830 (1997).

[11] K. Sakoda, *Optical Properties of Photonic Crystals* (Springer-Verlag, Berlin, 2001).

[12] E. N. Economou: *Green Functions in Quantum Physics* (Springer-Verlag, Berlin, 1983).

[13] A. A. Asatryan, K. Busch, R. C. McPhedran, L. C. Botten, C. M. de Sterke, and N. A. Nicorovici, Phys. Rev. E **63**, 046612 (2001).

[14] H. Y. Ryu, M. Notomi, G. H. Kim, and Y. H. Lee, Opt. Express **12**, 1708 (2004).